



Modeling of Leopard optimization based Node Localization Technique for Wireless Communication Networks

Manal M. Nasir^{1,*}, Salim M. Hebrisha²

¹Gwinnett Technical College (GTC), Lawrenceville , GA, 30043, USA

²Libyan Iron and Steel Company (LISCO), Misrata, Libya

Emails: Mnasir@gwinnettech.edu; salimhebrisha@gmail.com

Abstract

Wireless communication inculcates transfer of information not having any physical connection among two or more points. The significant operation of a sensor network becomes collecting and forwarding data to destiny. It is highly crucial to have an awareness regarding the place of collected data. This data is acquired by leveraging localization method in wireless sensor networks (WSNs). Localization is a way of determining the sensor nodes (SNs) location. Localization of SNs turns out to be an exciting research area, and several studies were performed till now. It is very favourable to model scalable, effectual, and low-cost localization systems for WSNs. This study develops a Leopard optimization based Node Localization Technique for Wireless Communication (LONLT-WC). The goal of the LONLT-WC model is to recognize the location of the nodes involved in the network. The LONLT-WC model involves the design of snow leopard optimization (SLO) algorithm, inspired from the characteristics of snow leopards. The presented LONLT-WC approach computes the unidentified location of the nodes utilizing anchor nodes in the network with the accomplishment of least error rate. The experimental analysis of the LONLT-WC model involves a series of simulations and the results highlighted the betterment of the presented technique.

Keywords: Wireless communication; Node localization; Snow leopard optimization; Wireless sensor networks; Anchor nodes

1. Introduction

The emerging pattern of computing and networking, wireless sensor networks (WSNs) were suitable in different fields like environmental control, medicine, military, surveillance, and climate forecasting, and much more. Constant advancements in network systems have importantly expanded and allowed wide implementation of WSNs. Currently, WSNs were combined with further ideas, such as the concept of the internet of things (IoT) [1]. A WSN is a network structure which comprises of large quantity of minuscule, cheap autonomous devices, diminutive, indicated as sensor nodes (SNs), that observe and identify the atmosphere for compiling information [2]. The information that is gathered from the atmosphere is transmitted subsequently to the sink node, a destiny in which information could be managed locally or transmitted to another networks for distinct practices [3]. Owing to its accessible placement, data transfer, self-organization, and node communications WSN have several developments and utilization, but it might also undergo few difficulties [4]. There comes several difficulties in WSNs' application procedure, like power utilization of (SNs), node localization, data routing issues coverage, and so on. In spite of all of these difficulties and problems, the important one is fixing the position of SNs [5]. With a view to gathering information from the atmosphere efficiently, the places or positions of every nodes need to be valid and well-known. Whether it is modified, the data could not be suited for other processes and utilization [6]. Fig. 1 showcases the overview of WSN.

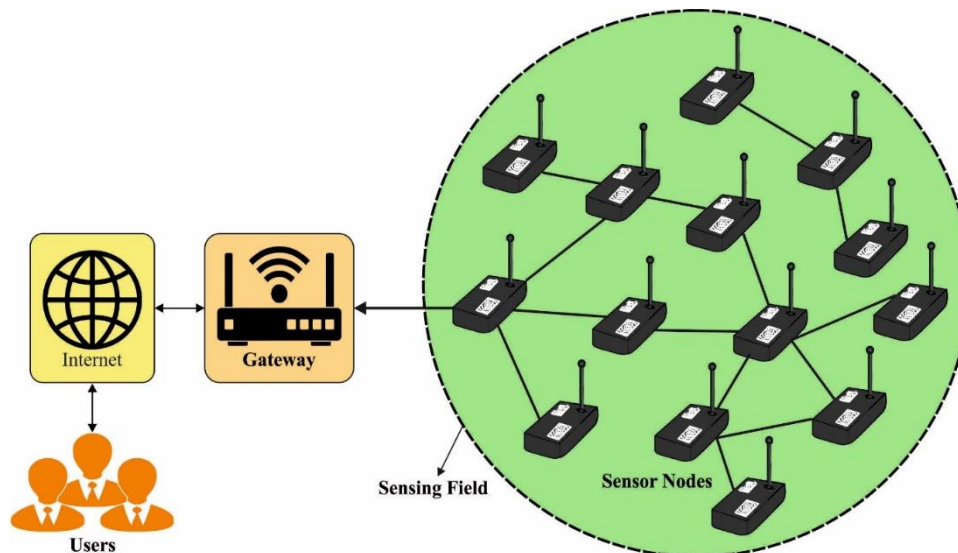


Figure1: Overview of WSN

Owing to the territory placement and diverse indoor environments and outdoor climates, few SNs could not be able to achieve, and in order to overcome this issue, there must be a connection and transmission system in which at each moment every SNs are evident and attained to collect and transfers information for forthcoming purposes [7]. There exit quite a few techniques which regard utilizing global positioning system (GPS) for each SNs which is positioned, but it may lead to malfunctioning of the sensors, power utilization for data transferring and node usage, along with the size and cost [8]. Concerning such difficulties and positioning form in atmosphere which is observed, the preferential substitute is localizing arranged nodes [9]. The WSNs localization issue is termed as the procedure of discovering correct localities of the strange target SNs which are deployed at a random way in the monitoring atmosphere by means of the prevailing accurate localities of SNs, represented as anchor nodes (ANs) [10], that is used for obtaining the positions and distance of target nodes (TNs) with the help of these methodologies like radio signal strength (RSS), triangulation, angle of arrival (AoA), time of arrival (ToA), and much more.

This study develops a Leopard optimization based Node Localization Technique for Wireless Communication (LONLT-WC). The goal of the LONLT-WC model is to recognize the location of the nodes involved in the network. The LONLT-WC model involves the design of snow leopard optimization (SLO) algorithm, inspired from the characteristics of snow leopards. The presented LONLT-WC approach computes the unidentified location of the nodes utilizing ANs in the network with the accomplishment of least error rate. The experimental analysis of the LONLT-WC model involves a series of simulations and the results highlighted the betterment of the presented technique.

2. Related works

Sekhar et al. [11] proposed an effective metaheuristic-related Group Teaching Optimization method for Node Localization (GTOA-NL) approach for WSN. The ultimate aim of GTOA-NL method was determining the location of the indefinite nodes using AN presented in WSN has maximal localizing accuracy and minimal localizing error. The proposed GTOA can be stimulated through group teaching scheme and utilized for optimizing procedure has no loss of generality. He et al. [12] present kernel regression to node localizing of anisotropic WSN that transforms the localizing issue into the kernel regression problem. Polynomial-kernel-related P-LSVR and Radial basis kernel-related G-LSVR have made a comparison with the traditional DV-Hop in anisotropic WSN as well as isotropic WSN in various proportion disturbances of communication range, beacons, and network scales. In [13], a node localizing technique was devised related to a new bioinspired approach known as Salp Swarm Algorithm (SSA). The presented method can be compared to familiar optimizing techniques, such as firefly algorithm (FA), PSO, GWO, and Butterfly optimization algorithm (BOA) in various WSN deployments.

A new node localization technique called Kernel Extreme Learning Machines depends on Hop count Quantization (KELM-HQ) can be projected in [14]. The recommended algorithm leverages the real number hop counts among unidentified nodes and anchors as trained inputs and the anchors places as

the trained targets for KELM training purposes. The modelled technique even uses the real number hop counts among indefinite nodes as test samples to calculate the indefinite nodes places by trained KELM. Amri et al. [15] modeled a fuzzy localization approach which employs flow measurement via wireless channel for computing the distance which separates the nodes and anchor. Then, this study depends on the centroid approach which computes the location of unidentified sensors leveraging Sugeno inference and fuzzy Mamdani mechanism to rise the accuracy of the estimated place. After detecting localization approach the nodes' location with unidentified location, the devised system chooses efficiently the next-elected CH for diminishing the energy dissipation of sensors, that results in an extension of the network lifespan.

3. The Proposed Localization Scheme

In this study, a new LONLT-WC technique has been developed to recognize the location of the nodes involved in the network. The LONLT-WC model involves the design of SLO algorithm, inspired by the characteristics of snow leopards.

3.1 Overview of SLO Algorithm

In this section, every snow leopard is member of the population. A specific amount of snow leopard as search agent is member of SLOA. In population- based optimization algorithm, population member is recognized by a matrix termed the population matrix [16]. The row number in the matrix is equivalent to the member number in the population, and the column number in this matrix is equivalent to the variable count of in the optimization issue and it is given in the following expression

$$X = \begin{bmatrix} X_1 \\ \vdots \\ X_i \\ \vdots \\ X_N \end{bmatrix} N \times m = \begin{bmatrix} X_{1,1} & \dots & X_{1,d} & X_1 X_{1,m} \\ \vdots & & \vdots & \vdots \\ X_i & & X_i & X_i X_i \\ \vdots & & \vdots & \vdots \\ X_N & & X_N & X_N X_N \end{bmatrix} N \times m \quad (1)$$

In Eq. (1), X refers to the population of snow leopards, X_i denotes the i^{th} snow leopards, $x_{i,d}$ denotes the value for d^{th} parameter recommended as i^{th} snow leopards, N indicates the snow leopard count, and m refers to the variable count of problem.

$$F = \begin{bmatrix} f_1 \\ \vdots \\ f_i \\ \vdots \\ f_N \end{bmatrix} = \begin{bmatrix} f(X_1) \\ \vdots \\ f(X_i) \\ \vdots \\ f(X_N) \end{bmatrix} \quad (2)$$

Now, F indicates the vector of objective function and F_i denotes the value for objective function of problem according to i^{th} snow leopards.

Member of population is upgraded according to the natural behavior of snow leopard in four stages: hunting, displacement, mortality, and reproduction. The arithmetical modelling of four stages and the stated nature behavior is given below.

Phase 1: Travel Routes and Movement

Snow leopards, similar to other cats, utilize scent signs to show the location and travel route. The sign is generally caused by scraping the ground with the hind feet beforehand dropping scat or urine. Also, snow leopard moves in a zig-zag pattern in indirect line. Consequently, snow leopard moves toward or follows one another according to nature behaviors.

This stage of the presented method is given as follows.

$$x_{i,d}^{P1} = x_{i,d} + r \times (x_{k,d} - I \times x_{i,d}) \times \text{sign}(F_i - F_k), \quad (3)$$

$$k \in 1,2,3, \dots, N, d = 1,2,3, \dots, m$$

$$X_i = \begin{cases} X_i^{P1}, & F_i^{P1} < F_i \\ X_i, & \text{else} \end{cases} \quad (4)$$

$$I = \text{round}(1 + r) \quad (5)$$

Now, $x_{i,d}^{P1}$ denotes the novel value for d -th problem variables attained through i -th snow leopards according to the stage 1, r represents an arbitrary value within $[0,1]$, k indicates the row count chosen snow leopards to guide i -th snow leopards in d -th axis, X_i^{P1} denotes the upgraded position of i -th snow leopards according to the stage 1, and F_i^{P1} represent the objective function value.

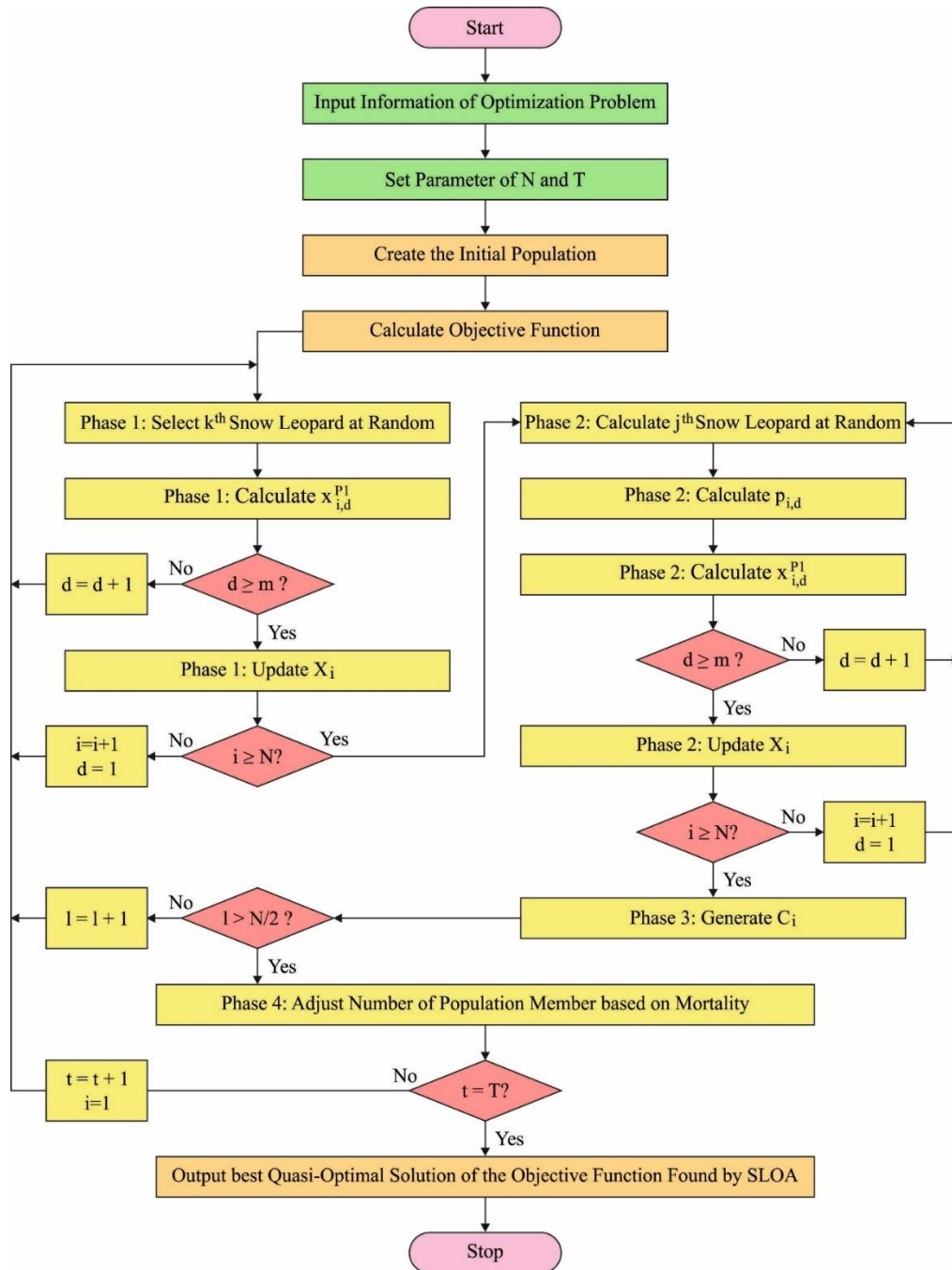


Figure 2: Flowchart of SLO technique

Phase 2: Hunting

In the following stage of upgrading the population member, the snow leopard behavior in attacking and hunting prey is applied. The novel location is satisfactory to the member when the value of objective function in the novel location is well suited than the preceding location.

$$p_{i,d} = x_{j,d}, d = 1, 2, 3, \dots, m \quad (6)$$

$$x_{i,d}^{P2} = x_{i,d} + r \times \left((p_{i,d} - x_{i,d}) \times P + (p_{i,d} - 2 \times x_{i,d}) \times (1 - P) \right) \quad (7)$$

$\times \text{sign}(F_i - F_p)$,

$$X_j = \begin{cases} X_i^{P2}, & F_i^{P2} < F_i \\ X_i, & \text{else} \end{cases} \quad (8)$$

Now, $p_{i,d}$ denotes the d -th dimension of position of prey assumed for i -th snow leopards, F_p represent the objective function value according to position of prey, $x_{i,d}^{P2}$ shows the novel value for d -th parameter attained through i -th snow leopards according to stage 2, and F_i^{P2} denotes the objective function.

Phase 3: Reproduction

Here, according to the natural reproductive behavior of snow leopard, novel members equivalent to half the overall population are included in the population. Indeed, it is considered that a cub is born according to the mating of snow leopard. The reproduction procedure of snow leopard is arithmetically modelled as follows

$$C_l = \frac{X_l + X_{N-l+1}}{2}, l = 1, 2, 3, \dots, \frac{N}{2} \quad (9)$$

Where, C_l indicates the l -th cub that is born from the mating of snow leopard.

Phase 4: Mortality

Living things are often in danger of dying. Even though reproduction rises the population of snow leopard, the snow leopard number remains unchanged because of losses and death. In the suggested model, it is considered that in every replication afterward reproduction, snow leopard faces mortality accurately as the puppies born number. Fig. 2 demonstrates the flowchart of SLO technique.

3.2 Process involved in LONLT-WC Technique

The LONLT-WC localization method was normally applied for evaluating the coordinates of SNs from WSN. The aim is to determine the coordinates of targeted node with minimalized major function [17]. The development of LONLT-WC methodology is shown below:

- i) Initialization of N undefined node and M AN at a random manner from the sensing region using transmission radius R . Every AN is defined for locating and sending the coordinates toward adjacent node. In all the iterations, the node that eventually solves is known as position node and the role as AN from the consecutive iteration.
- ii) The group of 3 or greater than 3 ANs occurs from the transmission radius was defined by location node.
- iii) The distance amongst the anchor and TNs were resolved and achieves dissimilar Gaussian noises. The targeted node computes the distance with $\hat{d}_i = d_i + n_i$ wherein d_i indicates the real distance that has determined amid the position of targeted nodes (x, y) and position of beacon (x_i, y_i) as follows:

$$d_i = \sqrt{(x - x_i)^2 + (y - y_i)^2} \quad (10)$$

- iv) Where n_i denotes the noise affecting the definite distance in $d_i \pm d_i \left(\frac{P_n}{100} \right)$ from which P_n shows the ratio of noise from the given distance.
- v) The TN is called a localized node once it encompasses 3 ANs in transmission range of targeted node. Because of trigonometric law of cosine or sine, the coordinates of targeted node were estimated.
- vi) The LONLT-WC method is worked to resolve the (x, y) coordinates of targeted node that minimize the localization error. The localization problem has average square distance amongst the anchor and TNs that are minimalized as follows:

$$f(x, y) = \frac{1}{N} \left(\sum_{i=1}^N \sqrt{(x - x_i)^2 + (y - y_i)^2} - \hat{d} \right)^2 \quad (11)$$

- vii) If $N \geq 3$ shows the AN count that transmission range.
- viii) A good measure (x, y) was evaluated by applying LONLT-WC technique final iteration.
- ix) The localization error was estimated to localized TN N_L . It is authenticated as average square of distance in solved node (X_i, Y_i) coordinates where the novel node coordinates (x_i, y_i) are given by:

$$E_L = \frac{1}{N_1} \sum_{i=1}^N \sqrt{(x_i - X_i)^2 + (y_i - Y_i)^2} \quad (12)$$

- x) Repeat 2-5 steps until the location of targeted node was identified. The localized method based on maximum localized errors E_1 and un-localization node count N_{N_L} are assessed through the employment of $N_{N_L} = M - N_L$. The minimal score of E_1 and N_{N_L} outcomes from localized efficiency.

4. Experimental Validation

This section investigates the performance of the LONLT-WC model under distinct aspects. Table 1 and Fig. 3 provide an extensive number of localized nodes (NOLON) examinations of the LONLT-WC model under distinct target nodes (TN) and anchor nodes (AN). The experimental values implied that the LONLT-WC model has shown enhanced results with maximum values of NOLON. For instance, with 25 TN and 10 AN, the LONLT-WC model has resulted in enhanced values of NOLON under each run. For instance, with run-1, the LONLT-WC model has shown improved NOLON of 23 whereas the EHO, HEHO, TGA, and DTGA models have shown reduced NOLON of 18, 19, 20, and 21 respectively. Moreover, with 50 TN and 15 AN, the LONLT-WC method has resulted in enhanced values of NOLON under each run. For example, with run-1, the LONLT-WC technique has shown improved NOLON of 50 whereas the EHO, HEHO, TGA, and DTGA approaches have portrayed reduced NOLON of 45, 47, 49, and 49 correspondingly. Furthermore, with 75 TN and 20 AN, the LONLT-WC algorithm has resulted in enhanced values of NOLON under each run. For example, with run-1, the LONLT-WC approach has shown improved NOLON of 73 whereas the EHO, HEHO, TGA, and DTGA algorithms have exhibited reduced NOLON of 68, 69, 70, and 71 correspondingly. Along with that, with 100 TN and 25 AN, the LONLT-WC model has resulted in enhanced values of NOLON under each run. For example, with run-1, the LONLT-WC model has displayed enhanced NOLON of 98 whereas the EHO, HEHO, TGA, and DTGA models have shown reduced NOLON of 93, 95, 97, and 97 correspondingly.

Table 1: NOLON analysis of LONLT-WC approach with existing approaches under distinct TN and AN

| Number of Localized Nodes | | | | | | | |
|---------------------------|-------------|----------------|-----------|-----------|-----------|-----------|-----------|
| Target Node | Anchor Node | No. of Runs | EHO | HEHO | TGA | Dyns-TGA | LONLT-WC |
| 25 | 10 | 1 | 18 | 19 | 20 | 21 | 23 |
| | | 2 | 17 | 19 | 21 | 23 | 24 |
| | | 3 | 21 | 22 | 23 | 23 | 24 |
| | | 4 | 18 | 19 | 20 | 22 | 24 |
| | | 5 | 19 | 21 | 23 | 24 | 25 |
| | | Average | 18 | 20 | 21 | 22 | 24 |
| 50 | 15 | 1 | 45 | 47 | 49 | 49 | 50 |
| | | 2 | 44 | 46 | 48 | 49 | 49 |
| | | 3 | 45 | 46 | 47 | 48 | 49 |
| | | 4 | 44 | 45 | 48 | 47 | 49 |
| | | 5 | 45 | 47 | 47 | 49 | 49 |
| | | Average | 44 | 46 | 47 | 48 | 49 |

| | | | | | | | |
|-----|----|----------------|-----------|-----------|-----------|-----------|-----------|
| 75 | 20 | 1 | 68 | 69 | 70 | 71 | 73 |
| | | 2 | 69 | 71 | 73 | 74 | 75 |
| | | 3 | 68 | 69 | 71 | 73 | 74 |
| | | 4 | 67 | 69 | 71 | 72 | 73 |
| | | 5 | 69 | 70 | 71 | 72 | 74 |
| | | Average | 68 | 67 | 71 | 72 | 73 |
| 100 | 25 | 1 | 93 | 95 | 97 | 97 | 98 |
| | | 2 | 94 | 96 | 97 | 98 | 99 |
| | | 3 | 94 | 95 | 96 | 96 | 98 |
| | | 4 | 92 | 93 | 95 | 97 | 99 |
| | | 5 | 92 | 93 | 95 | 96 | 98 |
| | | Average | 93 | 94 | 96 | 96 | 98 |

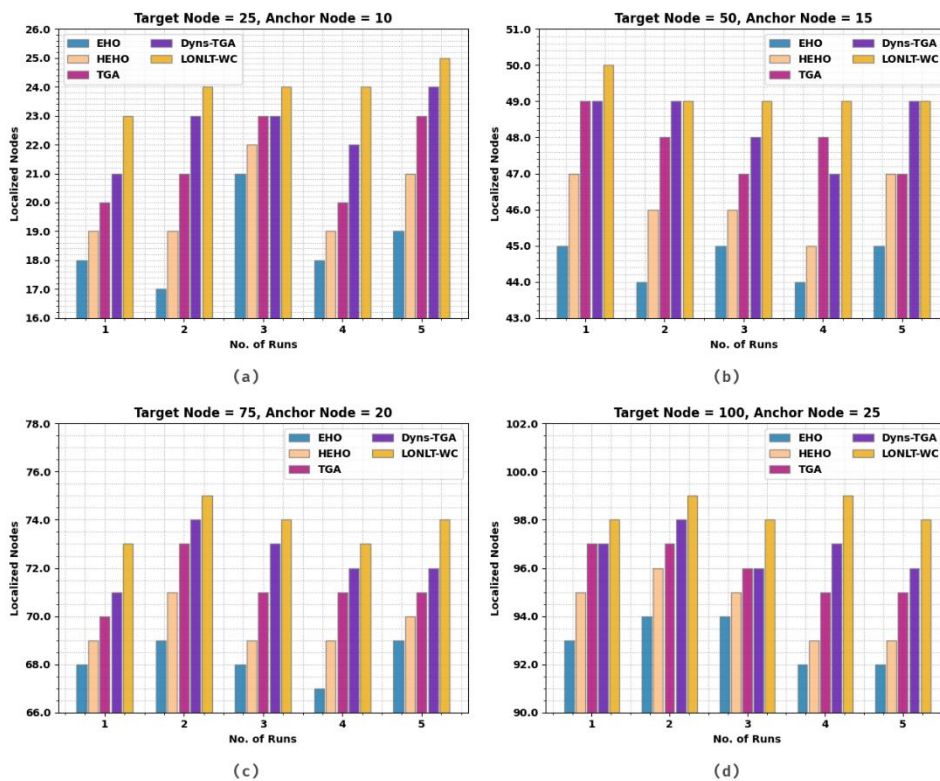


Figure 3: NOLON analysis of LONLT-WC approach (a) TN=25, AN=10, (b) TN=50, AN=15, (c) TN=75, AN=20, and (d) TN=100, AN=25

Fig. 4 portrays an average result of the LONLT-WC model interms of NOLON. With 25 TN and 10 AN, the LONLT-WC model has offered increased NOLON of 24 whereas the EHO, HEHO, TGA, and DTGA models have reported minimal NOLON of 18, 20, 21, and 22 respectively. Simultaneously, with 75 TN and 20 AN, the LONLT-WC method has rendered increased NOLON of 73 whereas the EHO, HEHO, TGA, and DTGA approaches have reported minimal NOLON of 68, 67, 71, and 72 correspondingly. Concurrently, with 100 TN and 25 AN, the LONLT-WC method has provided increased NOLON of 98 whereas the EHO, HEHO, TGA, and DTGA models have reported minimal NOLON of 93, 94, 96, and 96 correspondingly.

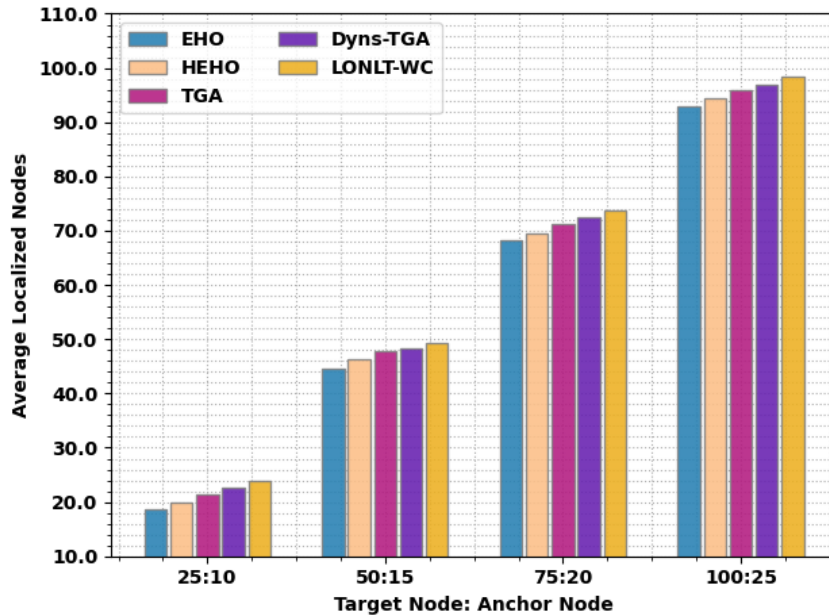


Figure 4: Average NOLON analysis of LONLT-WC approach with existing approaches

An extensive error rate (ER) inspection of the LONLT-WC model is tested with recent models under varying numbers of TNs and ANs in Table 2 and Fig. 5. With 25 TN and 10 AN, the LONLT-WC model has shown least values of ER under all runs. For instance, with run-1, the LONLT-WC model has obtained minimal ER of 0.0800 whereas the EHO, HEHO, TGA, and DTGA models have shown maximum ER of 0.2800, 0.2400, 0.2000, and 0.1600 respectively. In addition, with 75 TN and 20 AN, the LONLT-WC technique has shown least values of ER under all runs. For example, with run-1, the LONLT-WC approach has obtained minimal ER of 0.0267 whereas the EHO, HEHO, TGA, and DTGA models have shown maximum ER of 0.0933, 0.0800, 0.0667, and 0.0533 correspondingly. Likewise, with 100 TN and 25 AN, the LONLT-WC model has shown least values of ER under all runs. For example, with run-1, the LONLT-WC model has acquired minimal ER of 0.0200 whereas the EHO, HEHO, TGA, and DTGA models have shown maximum ER of 0.0700, 0.0500, 0.0300, and 0.0300 correspondingly.

Table 2: Error rate analysis of LONLT-WC approach with existing approaches under distinct TN and AN

| | | Error Rate | | | | | |
|-------------|-------------|----------------|---------------|---------------|---------------|---------------|---------------|
| Target Node | Anchor Node | No. of Runs | EHO | HEHO | TGA | Dyns-TGA | LONLT-WC |
| 25 | 10 | 1 | 0.2800 | 0.2400 | 0.2000 | 0.1600 | 0.0800 |
| | | 2 | 0.3200 | 0.2400 | 0.1600 | 0.0800 | 0.0400 |
| | | 3 | 0.1600 | 0.1200 | 0.0800 | 0.0800 | 0.0400 |
| | | 4 | 0.2800 | 0.2400 | 0.2000 | 0.1200 | 0.0400 |
| | | 5 | 0.2400 | 0.1600 | 0.0800 | 0.0400 | 0.0000 |
| | | Average | 0.2560 | 0.2000 | 0.1440 | 0.0960 | 0.0400 |
| 50 | 15 | 1 | 0.1000 | 0.0600 | 0.0200 | 0.0200 | 0.0000 |
| | | 2 | 0.1200 | 0.0800 | 0.0400 | 0.0200 | 0.0200 |
| | | 3 | 0.1000 | 0.0800 | 0.0600 | 0.0400 | 0.0200 |
| | | 4 | 0.1200 | 0.1000 | 0.0400 | 0.0600 | 0.0200 |
| | | 5 | 0.1000 | 0.0600 | 0.0600 | 0.0200 | 0.0200 |
| | | Average | 0.1080 | 0.0760 | 0.0440 | 0.0320 | 0.0160 |
| 75 | 20 | 1 | 0.0933 | 0.0800 | 0.0667 | 0.0533 | 0.0267 |
| | | 2 | 0.0800 | 0.0533 | 0.0267 | 0.0133 | 0.0000 |
| | | 3 | 0.0933 | 0.0800 | 0.0533 | 0.0267 | 0.0133 |

| | | | | | | | |
|-----|----|----------------|---------------|---------------|---------------|---------------|---------------|
| | | 4 | 0.1067 | 0.0800 | 0.0533 | 0.0400 | 0.0267 |
| | | 5 | 0.0800 | 0.0667 | 0.0533 | 0.0400 | 0.0133 |
| | | Average | 0.0907 | 0.0720 | 0.0507 | 0.0347 | 0.0160 |
| 100 | 25 | 1 | 0.0700 | 0.0500 | 0.0300 | 0.0300 | 0.0200 |
| | | 2 | 0.0600 | 0.0400 | 0.0300 | 0.0200 | 0.0100 |
| | | 3 | 0.0600 | 0.0500 | 0.0400 | 0.0400 | 0.0200 |
| | | 4 | 0.0800 | 0.0700 | 0.0500 | 0.0300 | 0.0100 |
| | | 5 | 0.0800 | 0.0700 | 0.0500 | 0.0400 | 0.0200 |
| | | Average | 0.0700 | 0.0560 | 0.0400 | 0.0320 | 0.0160 |

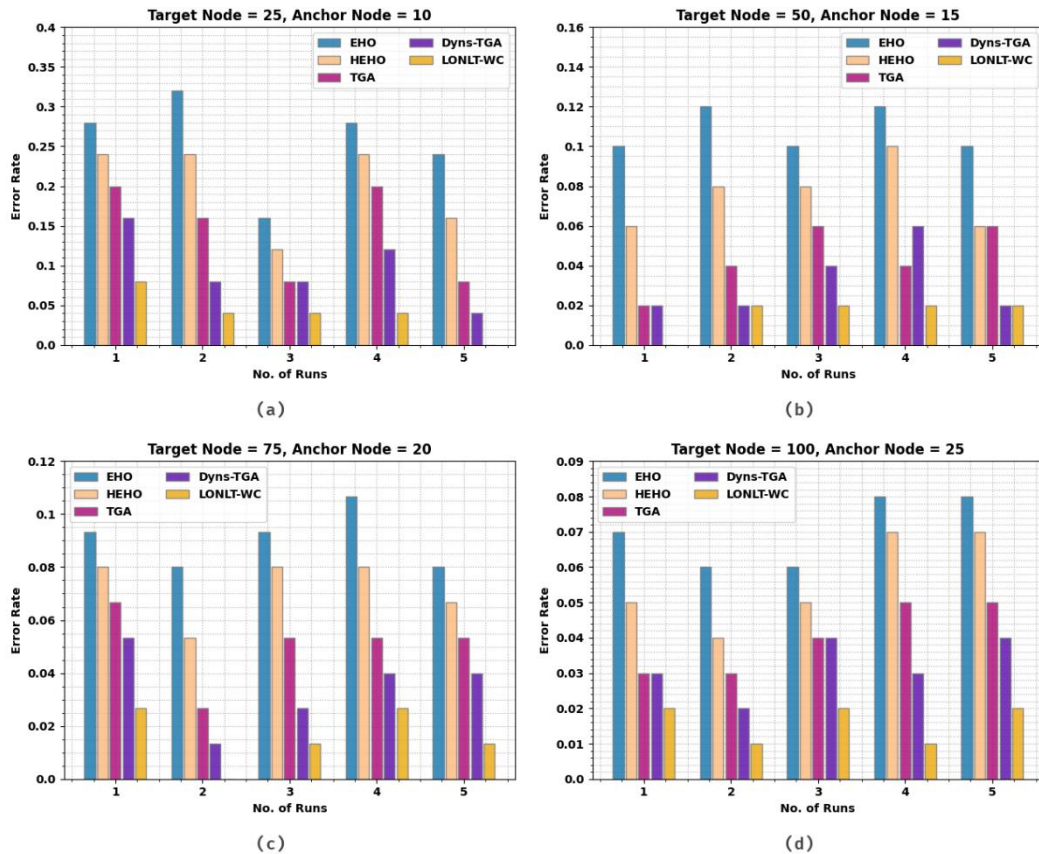


Figure 4: ER analysis of LONLT-WC approach (a) TN=25, AN=10, (b) TN=50, AN=15, (c) TN=75, AN=20, and (d) TN=100, AN=25

Fig. 6 depicts an average result of the LONLT-WC model interms of NOLON. With 25 TN and 10 AN, the LONLT-WC model has reported least ER of 0.0400 whereas the EHO, HEHO, TGA, and DTGA models have reported maximum ER of 0.2560, 0.2, 0.1440, and 0.0960 respectively. Simultaneously, with 75 TN and 20 AN, the LONLT-WC approach has reported least ER of 0.0160 whereas the EHO, HEHO, TGA, and DTGA models have reported maximum ER of 0.0907, 0.0720, 0.0507, and 0.0347 correspondingly. Concurrently, with 100 TN and 25 AN, the LONLT-WC technique has reported least ER of 0.0160 whereas the EHO, HEHO, TGA, and DTGA approaches have reported maximum ER of 0.0700, 0.0560, 0.0400, and 0.0320 correspondingly.

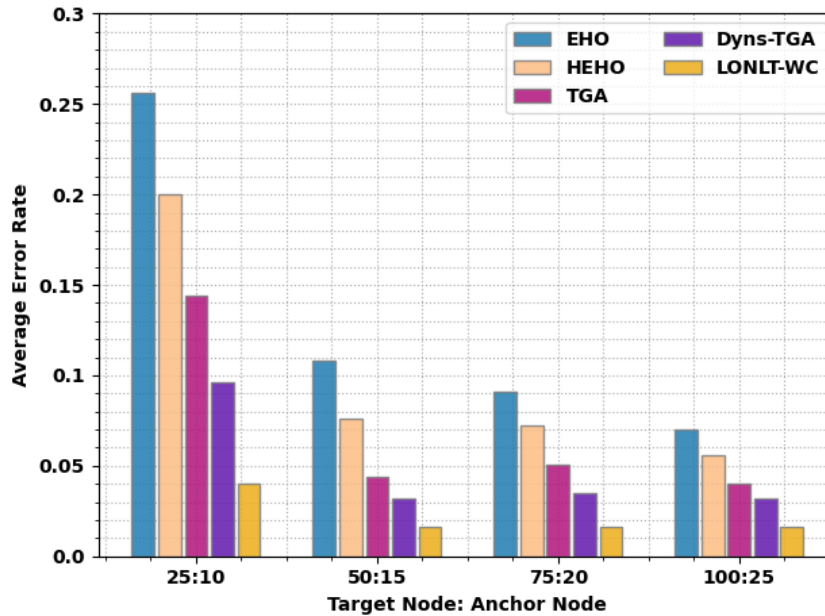


Figure 6: Average ER analysis of LONLT-WC approach with existing approaches

An extensive execution time (EXET) inspection of the LONLT-WC model is tested with recent approaches under varying numbers of TNs and ANs in Table 3 and Fig. 7. With 25 TN and 10 AN, the LONLT-WC method has shown least values of EXET under all runs. For instance, with run-1, the LONLT-WC model has acquired minimal EXET of 0.5780s whereas the EHO, HEHO, TGA, and DTGA algorithms have shown maximum EXET of 0.8741s, 0.8056s, 0.7365s, and 0.5780s correspondingly. Moreover, with 75 TN and 20 AN, the LONLT-WC model has shown least values of EXET under all runs. For example, with run-1, the LONLT-WC model has obtained minimal EXET of 1.4397s whereas the EHO, HEHO, TGA, and DTGA models have shown maximum EXET of 1.6972s, 1.6318s, 1.5766s, and 1.5180s correspondingly. Likewise, with 100 TN and 25 AN, the LONLT-WC model has shown least values of EXET under all runs. For example, with run-1, the LONLT-WC model has obtained minimal EXET of 1.5479s whereas the EHO, HEHO, TGA, and DTGA approaches have shown maximum EXET of 1.8512s, 1.7657s, 1.6948s, and 1.6340s correspondingly.

Table 3: Execution time analysis of LONLT-WC approach with existing approaches under distinct TN and AN

| Execution Time (sec) | | | | | | | |
|----------------------|-------------|----------------|---------------|---------------|---------------|---------------|---------------|
| Target Node | Anchor Node | No. of Runs | EHO | HEHO | TGA | Dyns-TGA | LONLT-WC |
| 25 | 10 | 1 | 0.8741 | 0.8056 | 0.7365 | 0.6497 | 0.5780 |
| | | 2 | 0.9482 | 0.8828 | 0.8264 | 0.7373 | 0.6527 |
| | | 3 | 1.0087 | 0.9345 | 0.8765 | 0.8064 | 0.7406 |
| | | 4 | 1.0803 | 1.0147 | 0.9343 | 0.8796 | 0.8084 |
| | | 5 | 1.1936 | 1.1078 | 1.0295 | 0.9601 | 0.8809 |
| | | Average | 1.0210 | 0.9491 | 0.8806 | 0.8066 | 0.7321 |
| 50 | 15 | 1 | 1.2687 | 1.2163 | 1.1437 | 1.0666 | 0.9916 |
| | | 2 | 1.3629 | 1.2943 | 1.2346 | 1.1625 | 1.1049 |
| | | 3 | 1.4733 | 1.4081 | 1.3393 | 1.2556 | 1.1668 |
| | | 4 | 1.5593 | 1.4810 | 1.4278 | 1.3704 | 1.3073 |
| | | 5 | 1.6307 | 1.5578 | 1.4767 | 1.4037 | 1.3179 |
| | | Average | 1.4590 | 1.3915 | 1.3244 | 1.2518 | 1.1777 |
| 75 | 20 | 1 | 1.6972 | 1.6318 | 1.5766 | 1.5180 | 1.4397 |
| | | 2 | 1.7819 | 1.7095 | 1.6309 | 1.5715 | 1.4980 |
| | | 3 | 1.8253 | 1.7545 | 1.6952 | 1.6425 | 1.5636 |
| | | 4 | 1.8131 | 1.7551 | 1.6968 | 1.6185 | 1.5461 |
| | | 5 | 1.7950 | 1.7239 | 1.6382 | 1.5612 | 1.4811 |
| | | Average | 1.7713 | 1.7018 | 1.6382 | 1.5612 | 1.4811 |

| | | Average | 1.7825 | 1.7150 | 1.6475 | 1.5823 | 1.5057 |
|-----|----|---------|--------|--------|--------|--------|--------|
| 100 | 25 | 1 | 1.8512 | 1.7657 | 1.6948 | 1.6340 | 1.5479 |
| | | 2 | 1.8899 | 1.8374 | 1.7603 | 1.7023 | 1.6447 |
| | | 3 | 2.0056 | 1.9197 | 1.8581 | 1.7882 | 1.7206 |
| | | 4 | 2.0113 | 1.9424 | 1.8555 | 1.7827 | 1.7293 |
| | | 5 | 2.1351 | 2.0451 | 1.9729 | 1.8974 | 1.8220 |
| | | Average | 1.9786 | 1.9021 | 1.8283 | 1.7609 | 1.6929 |

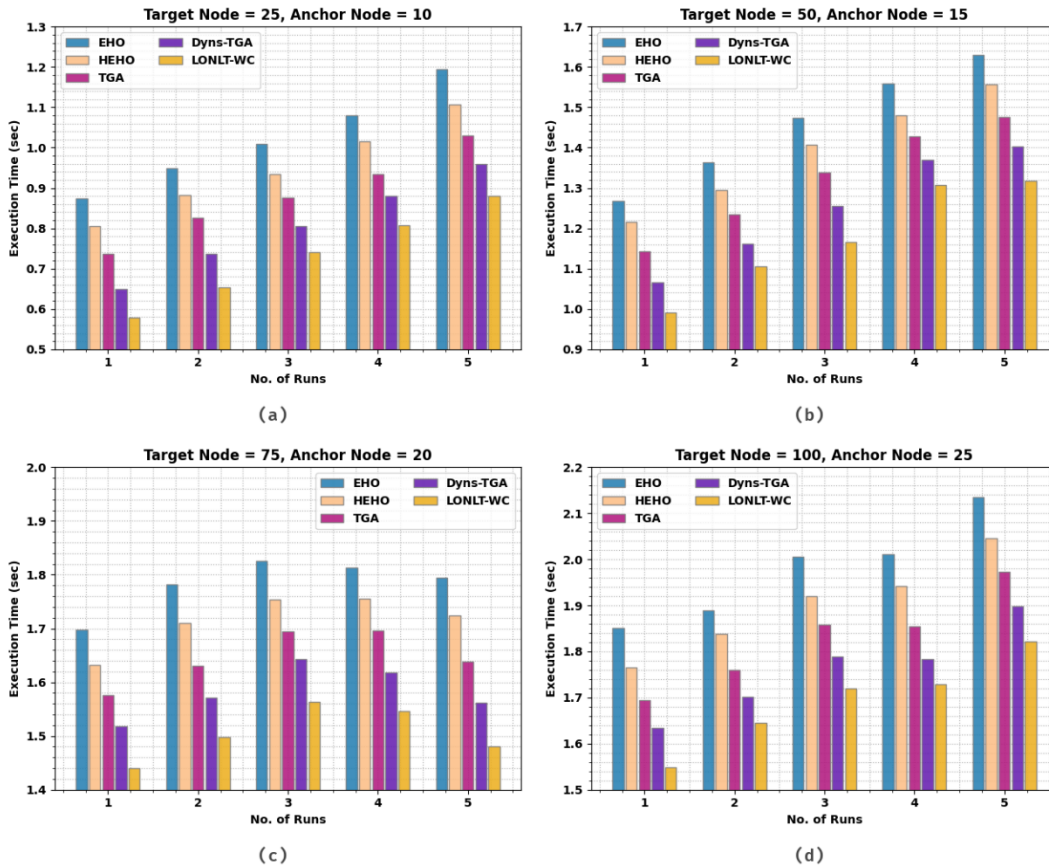


Figure 7: EXET analysis of LONLT-WC approach (a) TN=25, AN=10, (b) TN=50, AN=15, (c) TN=75, AN=20, and (d) TN=100, AN=25

Fig. 8 exhibits an average result of the LONLT-WC model interms of NOLON. With 25 TN and 10 AN, the LONLT-WC model has reported least EXET of 0.7321s whereas the EHO, HEHO, TGA, and DTGA approaches have reported maximum EXET of 1.0210s, 0.9491s, 0.8806s, and 0.8066s correspondingly. Concurrently, with 75 TN and 20 AN, the LONLT-WC model has reported least EXET of 1.5057s whereas the EHO, HEHO, TGA, and DTGA models have reported maximum EXET of 1.7825s, 1.7150s, 1.6475s, and 1.5823s correspondingly. Parallely, with 100 TN and 25 AN, the LONLT-WC model has reported least EXET of 1.6929s whereas the EHO, HEHO, TGA, and DTGA models have reported maximum EXET of 1.9786s, 1.9021s, 1.8283s, and 1.7609s correspondingly.

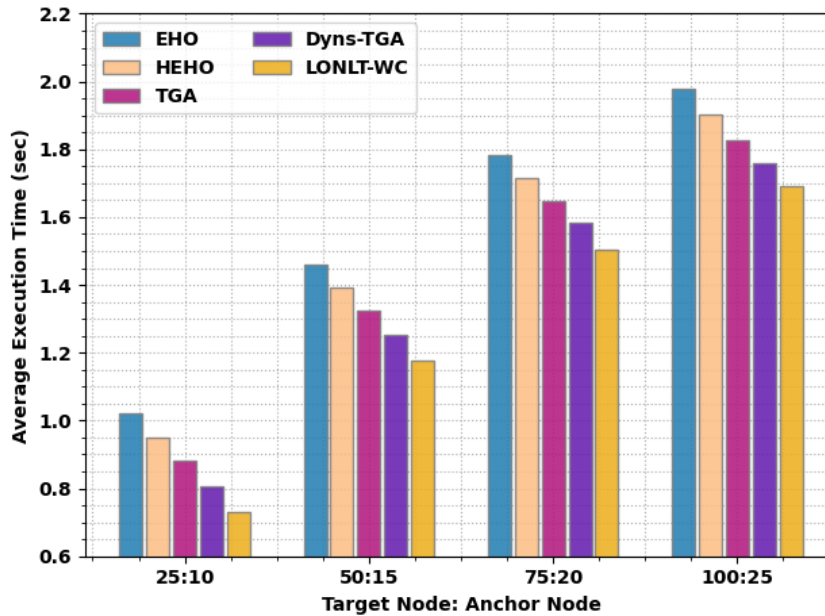


Figure 8: Average EXET analysis of LONLT-WC approach with existing approaches

5. Conclusion

In this study, a new LONLT-WC technique has been developed to recognize the location of the nodes involved in the network. The LONLT-WC model involves the design of SLO algorithm, inspired from the characteristics of snow leopards. The presented LONLT-WC approach computes the unidentified location of the nodes utilizing ANs in the network with the accomplishment of least error rate. The experimental analysis of the LONLT-WC model involves a series of simulations and the results highlighted the betterment of the presented technique. Thus, the LONLT-WC model can be utilized to attain enhanced localization efficiency over other models.

References

- [1] Sivasakthiselvan, S. and Nagarajan, V., 2020, July. Localization techniques of wireless sensor networks: A review. In 2020 International Conference on Communication and Signal Processing (ICCSP) (pp. 1643-1648). IEEE.
- [2] He, W., Cheng, R., Mao, K., Yan, K., Wei, J. and Xu, Y., 2022. A Novel Anchorless Node Positioning Method for Wireless Sensor Network. *Journal of Sensors*, 2022.
- [3] Sivasakthiselvan, S. and Nagarajan, V., 2019. A new localization technique for node positioning in wireless sensor networks. *Cluster Computing*, 22(2), pp.4027-4034.
- [4] El Khediri, S., Fakhret, W., Moulahi, T., Khan, R., Thaljaoui, A. and Kachouri, A., 2020. Improved node localization using K-means clustering for Wireless Sensor Networks. *Computer Science Review*, 37, p.100284.
- [5] Cheng, L., Hang, J., Wang, Y. and Bi, Y., 2019. A fuzzy C-means and hierarchical voting based RSSI quantify localization method for wireless sensor network. *IEEE Access*, 7, pp.47411-47422.
- [6] Vikram, R., Sinha, D., De, D. and Das, A.K., 2020. EEFFL: energy efficient data forwarding for forest fire detection using localization technique in wireless sensor network. *Wireless Networks*, 26(7), pp.5177-5205.
- [7] Kulkarni, V.R., Desai, V. and Kulkarni, R.V., 2019. A comparative investigation of deterministic and metaheuristic algorithms for node localization in wireless sensor networks. *Wireless Networks*, 25(5), pp.2789-2803.
- [8] Annepu, V. and Rajesh, A., 2020. Implementation of an efficient artificial bee colony algorithm for node localization in unmanned aerial vehicle assisted wireless sensor networks. *Wireless Personal Communications*, 114(3), pp.2663-2680.
- [9] Jin, Y., Zhou, L., Zhang, L., Hu, Z. and Han, J., 2022. A Novel Range-Free Node Localization Method for Wireless Sensor Networks. *IEEE Wireless Communications Letters*, 11(4), pp.688-692.

- [10] Walia, G.S., Singh, P., Singh, M., Abouhawwash, M., Park, H.J., Kang, B.G., Mahajan, S. and Pandit, A.K., 2022. Three Dimensional Optimum Node Localization in Dynamic Wireless Sensor Networks. *CMC-Computers, Materials & Continua*, 70(1), pp.305-321.
- [11] Sekhar, P., Lydia, E.L., Elhoseny, M., Al-Akaidi, M., Selim, M.M. and Shankar, K., 2021. An effective metaheuristic based node localization technique for wireless sensor networks enabled indoor communication. *Physical Communication*, 48, p.101411.
- [12] He, W., Lu, F., Chen, J., Ruan, Y., Lu, T. and Zhang, Y., 2021. A kernel-based node localization in anisotropic wireless sensor network. *Scientific Programming*, 2021.
- [13] Kanoosh, H.M., Houssein, E.H. and Selim, M.M., 2019. Salp swarm algorithm for node localization in wireless sensor networks. *Journal of Computer Networks and Communications*, 2019.
- [14] Wang, L., Er, M.J. and Zhang, S., 2020. A kernel extreme learning machines algorithm for node localization in wireless sensor networks. *IEEE Communications Letters*, 24(7), pp.1433-1436.
- [15] Amri, S., Khelifi, F., Bradai, A., Rachedi, A., Kaddachi, M.L. and Atri, M., 2019. A new fuzzy logic based node localization mechanism for wireless sensor networks. *Future Generation Computer Systems*, 93, pp.799-813.
- [16] Coufal, P., Hubálovský, Š., Hubálovská, M. and Balogh, Z., 2021. Snow leopard optimization algorithm: A new nature-based optimization algorithm for solving optimization problems. *Mathematics*, 9(21), p.2832.
- [17] Vojdani, M. and Dehghan, M., 2011. Localization in anchor less wireless sensor network. In *Proceedings of the International Conference on Computer Engineering and Applications (Vol. 2, pp. 365-369)*.